

A current-carrying coil design with improved liquid cooling arrangement

Leonardo Ricci, Luca Matteo Martini, Matteo Franchi, Andrea Bertoldi

▶ **To cite this version:**

Leonardo Ricci, Luca Matteo Martini, Matteo Franchi, Andrea Bertoldi. A current-carrying coil design with improved liquid cooling arrangement. Review of Scientific Instruments, 2013, 84, pp.065115. 10.1063/1.4811666 . hal-00995397

HAL Id: hal-00995397

https://hal-iogs.archives-ouvertes.fr/hal-00995397

Submitted on 18 Nov 2015

HAL is a multi-disciplinary open access archive for the deposit and dissemination of scientific research documents, whether they are published or not. The documents may come from teaching and research institutions in France or abroad, or from public or private research centers.

L'archive ouverte pluridisciplinaire **HAL**, est destinée au dépôt et à la diffusion de documents scientifiques de niveau recherche, publiés ou non, émanant des établissements d'enseignement et de recherche français ou étrangers, des laboratoires publics ou privés.

AIP | Review of Scientific Instruments

A current-carrying coil design with improved liquid cooling arrangement

Leonardo Ricci, Luca Matteo Martini, Matteo Franchi, and Andrea Bertoldi

Citation: Review of Scientific Instruments **84**, 065115 (2013); doi: 10.1063/1.4811666
View online: http://dx.doi.org/10.1063/1.4811666
View Table of Contents: http://scitation.aip.org/content/aip/journal/rsi/84/6?ver=pdfcov
Published by the AIP Publishing

Articles you may be interested in

Development of fast cooling pulsed magnets at the Wuhan National High Magnetic Field Center
Rev. Sci. Instrum. **84**, 125112 (2013); 10.1063/1.4849195

Efficient continuous-duty Bitter-type electromagnets for cold atom experiments
Rev. Sci. Instrum. **84**, 104706 (2013); 10.1063/1.4826498

Development of high resolution eddy current imaging using an electro-mechanical sensor
AIP Conf. Proc. **1430**, 324 (2012); 10.1063/1.4716246

On the magnetic field near the center of Helmholtz coils
Rev. Sci. Instrum. **81**, 084701 (2010); 10.1063/1.3474227

Modulated coil
Phys. Teach. **36**, 416 (1998); 10.1119/1.879909



This article is copyrighted as indicated in the article. Reuse of AIP content is subject to the terms at: http://scitationnew.aip.org/termsconditions. Downloaded to IP: 129.104.29.2 On: Mon, 19 Oct 2015 09:16:14

A current-carrying coil design with improved liquid cooling arrangement

Leonardo Ricci,[a] Luca Matteo Martini, Matteo Franchi, and Andrea Bertoldi[b]
Dipartimento di Fisica, Università di Trento, I-38123 Trento, Italy

(Received 11 April 2013; accepted 6 June 2013; published online 27 June 2013)

The design of an electromagnet requires the compliance with a number of constraints such as power supply characteristics, coil inductance and resistance, and, above all, heat dissipation, which poses the limit to the maximum achievable magnetic field. A common solution consists in using copper tubes in which a coolant flows. This approach, however, introduces further hydrodynamic concerns. To overcome these difficulties, we developed a new kind of electromagnet in which the pipe concept is replaced by a duct formed by the windings. Here we report on the realization and characterization of a compact model system in which the conductors carry a current that is one order of magnitude higher than the current allowable with conventional designs. © *2013 AIP Publishing LLC*. [http://dx.doi.org/10.1063/1.4811666]

I. INTRODUCTION

The inductance and resistance of the coils, the volume available for the conductors, the operation temperature, and the characteristics of the power supply are among the most crucial constraints to comply with when designing an electromagnet. A prototypical situation is illustrated in Fig. 1: a toroidal region of given volume hosts the current-carrying wires to generate a magnetic field in the configuration center O. According to the Biot-Savart law, the axial component B of this field is given by

$$B \simeq \frac{\mu_0}{2}\frac{J \cdot S}{r},$$

where J is the average current density flowing through the toroidal cross-section S, and r is the torus radius. Therefore, if the geometry is assigned, the maximum B is proportional to the maximum J compatible with heat dissipation. If a coil is made of N windings, in which a current I is flowing, one has

$$I \simeq \frac{J \cdot S}{N}, \quad R \simeq \rho\frac{2\pi r}{S}N^2,$$

where ρ is the conductor resistivity (incidentally, the inductance also increases as N^2). The relationship between J and the dissipated power P is given by $P \simeq \rho V J^2$ or, equivalently, by

$$J \simeq \sqrt{\frac{P}{\rho V}},$$

where $V \simeq 2\pi r S$ is the volume occupied by the conductors.[1]

The maximum J and, consequently, the maximum achievable B are then independent of I and N and proportional to the square root of the maximum P, which is, on its part, set by the maximum possible operation temperature (to a first approximation, the resistivity ρ and the volume V are supposed to be temperature-independent). Typically, a copper conductor can carry a maximum J of several A mm^{-2}.

Improving heat dissipation is then crucial to enhance the magnetic field provided by an electromagnet.[2–6] A popular solution consists in using copper tubes with a cylindrical bore in which a coolant (typically water) flows.[7–9] This solution, however, introduces further design concerns due to the viscous resistance $\mathcal{R}$ that is opposed by the pipe to the coolant flow,[10] and the dependence of $\mathcal{R}$ on the pipe length L and bore cross-section σ. For example, in the case of a laminar flow, $\mathcal{R}$ scales as σ^{-2}. Since L and σ are proportional to the number of windings N and its reciprocal N^{-1}, respectively, the viscous resistance scales as N^3: consequently, increasing the number of windings (for example, in order to reduce the current) is detrimental for power dissipation. In principle, any desired value of coolant flow could be achieved by suitably setting the coolant pressure. However, increasing this parameter requires a number of technical artifices – for example, special pumps and fittings – that make this solution inconvenient, if not unfeasible.

To overcome this difficulty posed by hydrodynamics, we developed a new kind of water-cooled electromagnet in which the windings form a rectangular duct. Section II describes the structure of the magnet, whereas the tests carried out on the magnet are discussed in Sec. III.

II. STRUCTURE OF THE MAGNET

Our magnet (see Fig. 2) is composed by two coils, henceforth, referred to as the back and the front coil. The back coil is made of 5 windings. The windings were produced out of a copper bulk by means of electric discharge machining, and are held together by a thermally conductive epoxy (Epo–Tek H77) that fills the 0.5 mm wide spacing between them.

In the case of the four innermost windings no. 2–5, the current-carrying conductor has a rectangular cross section, 3 mm wide and 2 mm thick. The outermost winding no. 1 and the inner part of the coil (*central pad*, see Fig. 2) are 3.25 mm thick. In this way, a cavity is formed which is 16.25 mm wide and 1.25 mm deep. Rather than being a ring, this cavity is "C-shaped" due to a tiny wall formed by four 1.25 mm thick bulges on the transitions between consecutive windings, and an additional bulge placed at the *end pad* of winding no. 1. In the right bottom part of winding

[a] ricci@science.unitn.it
[b] Also at Laboratoire Photonique, Numérique et Nanosciences - LP2N, Université Bordeaux 1, F-33405 Talence, France.

 © 2013 AIP Publishing LLC

This article is copyrighted as indicated in the article. Reuse of AIP content is subject to the terms at: http://scitationnew.aip.org/termsconditions. Downloaded to IP: 129.104.29.2 On: Mon, 19 Oct 2015 09:16:14

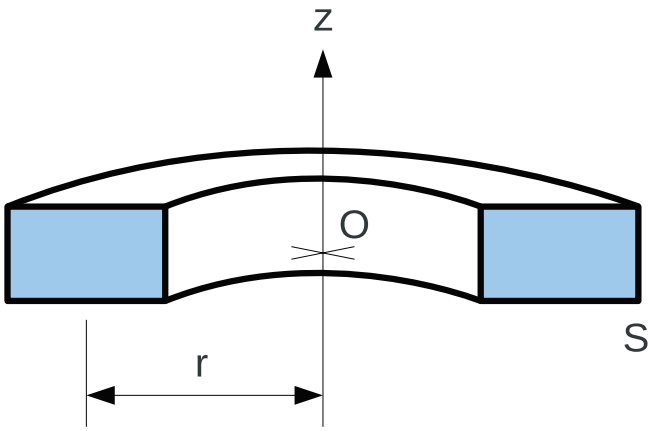


FIG. 1. A fixed toroidal region hosts the current-carrying wires.

no. 1, the coil shows a 6.5 mm thick, pentagonal bulge with a M6×1 female thread that is used for the electrical connection. A set of ten clearance holes of ø = 1.2 mm are placed in the outermost winding no. 1.

The front coil is identical to the back coil except for the following five features:

1. The central pad of the back coil contains a 3.25 mm thick square bulge that precisely fits into the central square hole in the front coil (side of the square equal to 16 mm).
2. The center of the back coil hosts a M6×1 female thread that can be used to hold the magnet.
3. The 1.25 mm and 3.25 mm measures that characterize the thickness of several elements in the back coil are, respectively, reduced to 1.15 mm and 3.15 mm in the case of the front coil.

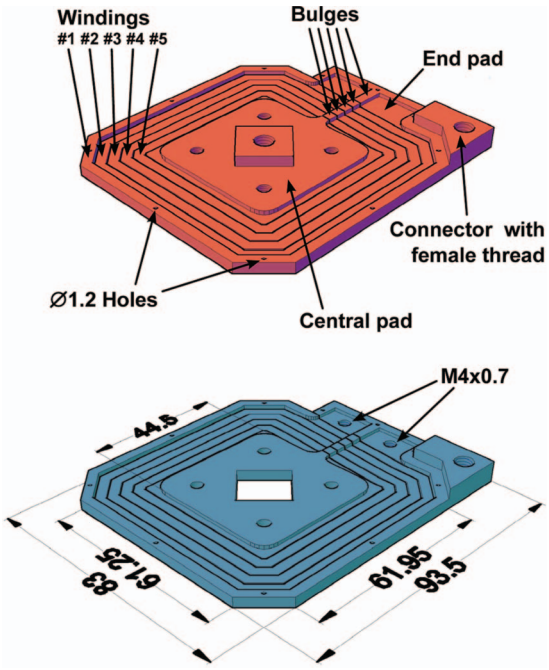


FIG. 2. Oblique perspective projection of the back (top, red) and the front (bottom, blue) coil. The lower sides of the two coils (not shown) are flat. Relevant sizes are shown. The structures of the two coils are described in detail in the main text.

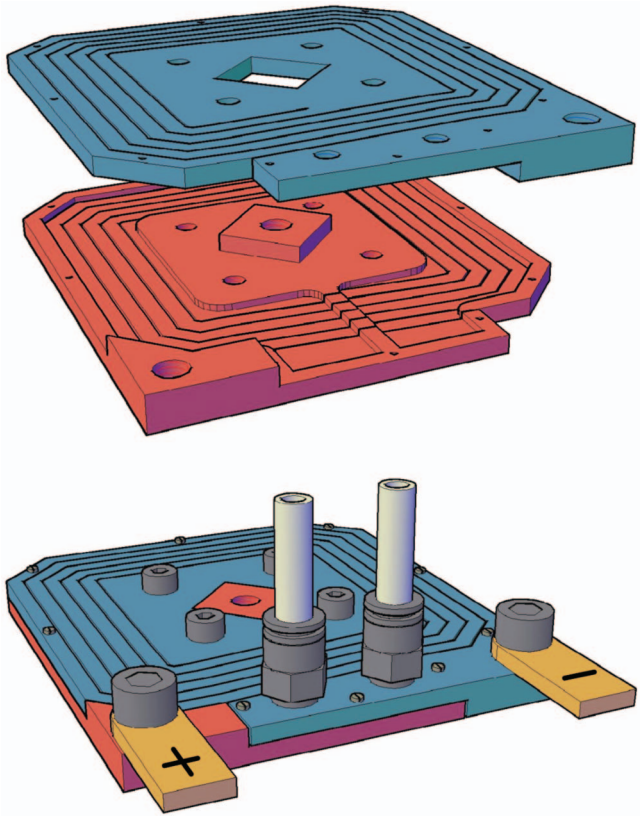


FIG. 3. Assembly of the two coils (top) to form the final magnet (bottom). The artist's view of the magnet also shows the tightening screws, the electric connections, and the quick release hydraulic couplings with related tubes (Rilsan®; outer ø = 6 mm, inner ø = 4 mm).

4. The central pad of the back coil hosts four clearance holes of ø = 4 mm, whereas the corresponding four holes in the central pad of the front coil are threaded (M4×0.7).
5. The end pad of the front coil hosts two M4×0.7 female threads for the insertion of quick release hydraulic couplings.

The magnet is assembled by putting the two coils into contact, so that the central square bulge in the back coil coincides with the central square hole in the front coil (see Fig. 3). Between the two coils, a thin (≈0.1 mm thick; see point 3 of the list above regarding the differences between the two coils) layer of Teflon® or similar sealing materials (e.g., Arexons Motorsil) is placed. Finally, the structure is tightly closed, first, by tightening four stainless steel M4×0.7 screws through the correspondent clearance and threaded holes in the central pads, and, second, by tightening ten stainless steel, electrically isolated M1×0.25 screws placed through the clearance holes (ø = 1.2 mm) in the outermost windings of the two coils. The electrical isolation of these screws is achieved by inserting them within a nonconductive polymeric tubing (for example, heat shrinkable tubing or Teflon®) and using Teflon® washers. The four M4×0.7 tightening screws also provide the electrical connection between the two coils.

Assuming that winding no. 1 of the back coil is connected to the positive pole of a power supply, the current enters the back coil and flows clockwise to the central pad. From here

This article is copyrighted as indicated in the article. Reuse of AIP content is subject to the terms at: http://scitationnew.aip.org/termsconditions. Downloaded to IP: 129.104.29.2 On: Mon, 19 Oct 2015 09:16:14

it flows through the four M4 screws to the front coil's central pad and finally, again clockwise, to the connector on the front coil's winding no. 1.

III. TEST OF THE MAGNET

The magnet resistance was measured by using a multimeter (Agilent 34410A) connected in four-wire configuration: the resistance at room temperature (20 °C) is 6.362(2) mΩ, very close to the value of 6.26 mΩ calculated by considering the magnet geometry and assuming a copper resistivity of 1.68×10^{-8} Ω m. The inductance was measured to be 6.3 μH.

To test the magnet, we implemented the setup described in Fig. 4. The magnet is fed by a power supply through a shunt resistance R. To measure the current, the voltage drop across R is measured by means of a multimeter (Agilent 34410A). The values of the two shunts used in the test phase were measured by using two multimeters (Agilent 34410A) and a current source (Agilent E3649A). With regard to the hydraulic part, a flowmeter (Parker Hannifin DFC9000100) and a pressure sensor (Freescale Semiconductor MPX5100) measure the upstream water flow and pressure. The upstream water temperature is instead measured by means of a PT100 gauge, whose resistance value is read by a multimeter (Agilent 34410A) connected in four-wire configuration. An identical configuration is used to measure the temperature on the surface of the magnet near the water outlet, i.e., at the warmest region of the device.[11] Finally, the axial component of the magnetic field produced by the magnet is measured by using a magnetoresistive magnetometer[12,13] that uploads the readouts to a personal computer (PC). The magnetometer head is placed on the magnet axis at a distance z above its center.

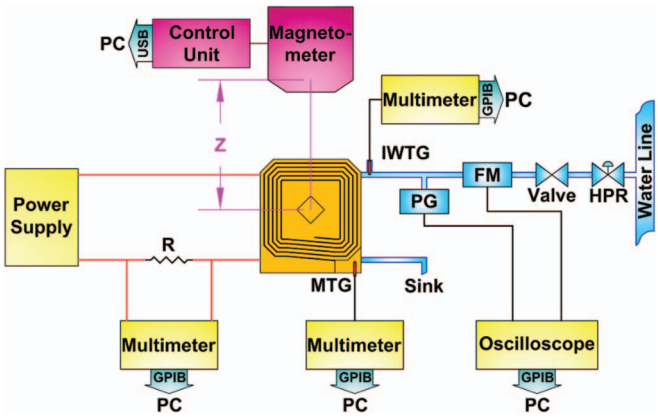


FIG. 4. Measurement setup. Electric part (left and bottom): A power supply is connected to the magnet through a shunt resistance R in order to measure the current. Hydraulic part (right): Water, collected from the laboratory line, flows through a hydraulic pressure regulator (HPR) and a valve. Before entering the magnet, water flow, pressure, and temperature are measured via a flowmeter (FM), a pressure sensor (PG), and a PT100 gauge (input water temperature gauge, IWTG), respectively. An additional PT100 gauge (magnet temperature gauge, MTG) is used to measure the temperature on the surface of the magnet near the water outlet. Magnetic part (top): The axial component of the magnetic field produced by the magnet at a distance z above its center is measured by using a magnetoresistive magnetometer.

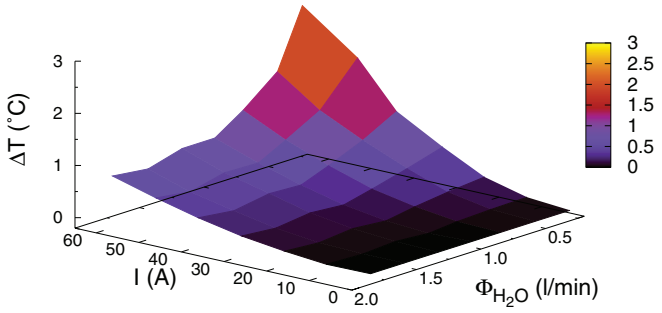


FIG. 5. Magnet temperature increase ΔT, with respect to the pipe temperature (≈15 ± 2) °C, as a function of current I and water flux Φ_{H_2O}. As expected, ΔT is proportional to I^2 and inversely proportional to Φ_{H_2O}. The temperature was measured after setting I and Φ_{H_2O} and waiting for a suitable thermalization time (5 min). The current was provided by the DC power supply. At the maximum current of 60 A (corresponding to a dissipated power of 22 W), and with a flux of 0.3 l/min, the temperature increase was less than 3 °C.

For a first characterization of the magnet, a DC power supply (Agilent 6573A) working between 0 and 60 A (0–35 V, 2100 W) was used. The shunt resistance R was 447(3) $\mu\Omega$. Figure 5 shows the magnet temperature increase as a function of current I (up to 60 A) and water flux Φ_{H_2O} (from 0.3 to 1.9 l/min). At the same time, we also measured the magnetic field B by means of a magnetometer head placed at a distance $z = 95(1)$ mm above the magnet center. As shown in Fig. 6, the axial magnetic field at the magnetometer head grows as 8.055(2) μT/A. This value coincides within the experimental error with the value of 8.1(2) μT/A calculated by considering the magnet geometry and using the Biot-Savart law (the error of 0.2 μT/A is due to the uncertainty on z).

The magnet operation was then tested at much higher current and power by using a home-made AC power supply that provides up to 500 A (6 V, 50 Hz). The shunt resistance R was 90(2) $\mu\Omega$. The magnetometer head was placed at two different distances above the magnet center, namely, $z = 200(1)$ mm and $z = 240(1)$ mm, in order not to saturate the magnetoresistive sensor. For both z-positions, the graph of the rms magnetic field as a function of the rms current is also plotted

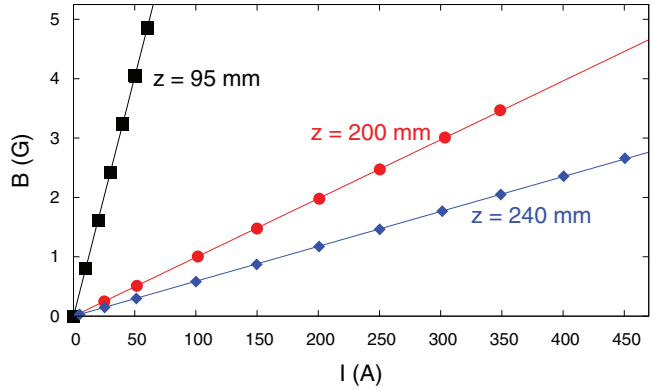


FIG. 6. Axial component of the magnetic field measured by the magnetoresistive magnetometer as a function of the current. Three different graphs are plotted, each corresponding to a different position z of the sensor with respect to the magnet. The best-fit straight lines to the points are also shown. For the last two positions, the AC power supply (50 Hz) was used, and the reported current and magnetic field values are rms.

This article is copyrighted as indicated in the article. Reuse of AIP content is subject to the terms at: http://scitationnew.aip.org/termsconditions. Downloaded to IP: 129.104.29.2 On: Mon, 19 Oct 2015 09:16:14

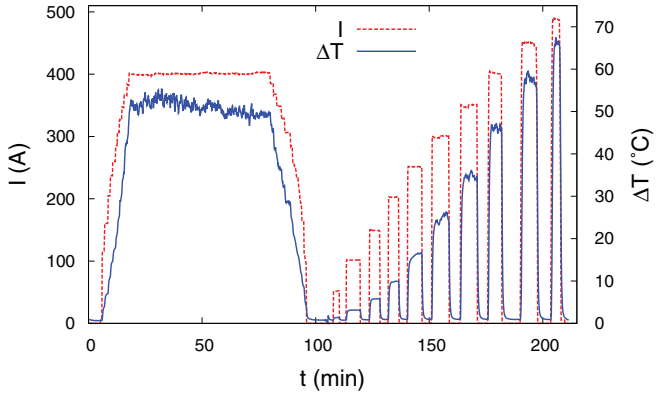


FIG. 7. Magnet temperature increase (blue, solid line), with respect to the pipe temperature ($\approx 13 \pm 1$) °C, as a function of time and in case of a varying current (red, dashed line) flowing through the magnet. During the first 100 min of *normal operation*, the water flux was 1.2 l/min; during the last 100 min of *stress test*, the water flux was 1.3 l/min. All measurements reported in this figure were carried out by using the AC power supply (50 Hz); the current values are rms.

in Fig. 6. The fitted field-to-current ratios (B/I) are 0.991(1) μT/A and 0.5877(7) μT/A, respectively. These values are also consistent with the predicted ones, equal to 1.03(2) μT/A and 0.608(8) μT/A, respectively.

During the first phase (*normal operation*; see Fig. 7), the current was ramped up in 18 min to a value of 400 A. The current was then kept constant for about 60 min after which the current was ramped down to zero in 18 min. During the second phase (*stress test*; see Fig. 7), that also lasted about 100 min, the current was switched on and off for 10 cycles. The switch-time was less than 10 s, thus much shorter than the thermal time scale. The current in the nth cycle is $n \cdot 50$ A, so that during the last cycle a value of 500 A was reached. Although the 500 A current used in this last test, corresponding to a dissipated power of about 2 kW (copper temperature ≈80 °C), overcomes by at least a factor 10 the maximum allowable current for a conductor of cross-sectional area equal to 6 mm^2 (see, for example, Refs. 14 and 15), the magnet did not suffer significant failures.

The forced convection heat transfer rate $\dot{Q}$ from the copper bulk to the flowing water is given by Newton's law of cooling, $\dot{Q} = hA(T_{Cu} - T_{H_2O})$, where h is the forced convection heat transfer coefficient, A is the area of the interface between copper and water (in the case of our magnet, $A \approx 95$ cm^2), and T_{Cu}, T_{H_2O} are the average copper and water temperatures, respectively. Because copper is an excellent heat conductor and the water inlet and outlet are very close, T_{Cu} is assumed to be uniform. Given the water flux value used in the first phase (1.2 l/min), we estimate $hA \approx 30$ W K^{-1} at $T_{H_2O} = 20$ °C; the quantity hA increases linearly with T_{H_2O} at a rate of about 0.32 W K^{-1}/K. If we also assume that all the dissipated heat is transferred to water ($\dot{Q} = P$), then, given the other experimental conditions of the first phase ($P = 1.19$ kW, upstream water temperature of 13 °C, magnet temperature increase of 50 °C), we can estimate an average water temperature increase of 11 °C and thus a final water temperature of 35 °C.

The design discussed in this paper is particularly suitable to be implemented in setups for the generation of high-gradient or high-curvature magnetic fields.[16] This is mainly due to the fact that it is possible to develop magnets that are thinner than those built by wrapping copper tubes. For example, our magnet produces a maximum gradient per unit current of 42 mT/(A m) at a distance of 14 mm from the magnet surface; the maximum curvature per unit current, occurring at the magnet center, is 45 T/(A m^2). At a distance of 30 mm, for example, the two quantities drop to 28 mT/(A m) and 11 T/(A m^2), respectively. Although the magnet design was not optimized with respect to gradient and curvature, these values are comparable with those reported for conventional magnetic traps for neutral atoms that rely on copper tubes.[17] Finally, our design approach and the use of electric discharge machining allow for precisely tailoring the coils and achieving flat structures.

ACKNOWLEDGMENTS

We thank Alberto Manfredi of Sama Meccanica, Rovereto, Italy for useful discussions and help concerning the machining of the coil.

[1] F. Bitter, Rev. Sci. Instrum. **7**, 482 (1936).
[2] K. Bessho, S. Yamada, M. Kooto, M. Masahashi, and M. Nakano, J. Appl. Phys. **64**, 6020 (1988).
[3] P. Rub and W. Joss, IEEE Trans. Magn. **32**, 2570 (1996).
[4] O. Lips, A. Privalov, S. Dvinskikh, and F. Fujara, J. Magn. Reson. **149**, 22 (2001).
[5] J. Leggett, S. Crozier, and R. W. Bowtell, J. Magn. Reson. **165**, 196 (2003).
[6] J. Smolka and A. J. Nowak, IEEE Trans. Magn. **47**, 1726 (2011).
[7] F. Bitter, Rev. Sci. Instrum. **10**, 373 (1939).
[8] F. Bitter, Rev. Sci. Instrum. **33**, 342 (1962).
[9] M. Dhotre, Z. Murthy, and N. Jayakumar, Chem. Eng. J. **118**, 183 (2006).
[10] L. F. Moody, Trans. ASME **66**, 671 (1944).
[11] E. Odvářka, N. L. Brown, A. Mebarki, M. Shanel, S. Narayanan, and C. Ondrůšek, in *5th IET International Conference on Power Electronics, Machines and Drives* (PEMD 2010), p. 414.
[12] A. Bertoldi, D. Bassi, L. Ricci, D. Covi, and S. Varas, Rev. Sci. Instrum. **76**, 065106 (2005).
[13] A. Bertoldi, L. Botti, D. Covi, R. Buffa, D. Bassi, and L. Ricci, Eur. Phys. J.: Appl. Phys. **33**, 51 (2006).
[14] ISO, "ISO 10133:2000(E), Small craft – Electrical systems – Extra-low-voltage dc installations", Technical Report (International Organization for Standardization, 2000).
[15] ISO, "ISO 13297:2000(E), Small craft – Electrical systems – Alternating current installations", Technical Report (International Organization for Standardization, 2000).
[16] L. Ricci, A. Bertoldi, and D. Bassi, Rev. Sci. Instrum. **73**, 3181 (2002).
[17] C. Fort, M. Prevedelli, F. Minardi, F. S. Cataliotti, L. Ricci, G. M. Tino, and M. Inguscio, Europhys. Lett. **49**, 8 (2000).

This article is copyrighted as indicated in the article. Reuse of AIP content is subject to the terms at: http://scitationnew.aip.org/termsconditions. Downloaded to IP: 129.104.29.2 On: Mon, 19 Oct 2015 09:16:14